

NUMERICAL STUDY ON THE EFFECT OF MERIDIONAL WIDTH VANED DIFFUSER ON THE PERFORMANCE OF A MODIFIED CENTRIFUGAL FLOW COMPRESSOR

Layth H. Jawad

Department of Mechanical Techniques, Technical Institute of Karbala,
Al-Furat Al-Awsat Technical University, IRAQ
Email: laihasan@yahoo.com

ABSTRACT

In This paper, a numerical simulation that was made in the three-dimensional flow, carried out in a modified centrifugal compressor, having vaned diffuser stage, used as an automotive turbo charger. In order to study the influence of vaned diffuser meridional outlet section with a different width ratio on the modified centrifugal compressor. Moreover, the performance of the centrifugal compressor was dependent on the proper matching between the compressor impeller along with vaned diffuser. In addition, the curves of polytropic efficiency, total pressure ratio, static pressure and aerodynamic characteristics were compared under different width ratio. In addition, the velocity vectors in diffuser flow passages, the absolute Mach number and the secondary flow in cross-section near the outlet of diffuser were analyzed in detail under width ratio of 0.5, 0.7, 0.8, 1 and 1.2. Another aim of this research was to study and simulate the effect of vaned diffuser on the performance of a centrifugal compressor. The simulation was undertaken by using CFD analysis on aerodynamic flow to predict numerically the performance in terms of pressure ratio, polytropic efficiency and mass flow rate for the centrifugal compressor stage. The results were generated from CFD (ANSYS CFX) and were analyzed for better understanding of the fluid flow through centrifugal compressor stage and as a result when the width ratio is 0.5, the flow in diffuser passages tends to be uniformity. The backflow and vortex near the pressure surface disappear, and the vortex and detachment near the suction surface decrease. Conclusively, it was observed that the efficiency was increased and both the total pressure ratio and static pressure for 0.5 width ratio are increased.

KEYWORDS: Numerical Study; Centrifugal Compressor Performance; Vaned Diffuser; CFD.

دراسة عددية على تأثير العرض الطولي لناشر ذي ريش على أداء جريان الضاغط الطرد المركزي المطور

الخلاصة

في هذه البحث تم اجراء دراسة عددية لتدفق ثلاثي الأبعاد، نفذت في طور ضاغط الطرد المركزي المطور ، مع ناشر ذي ريش، تم استخدامه كشاحن تربيني للسيارات . من أجل دراسة تأثير مقطع الخروج الطولي لناشر ذي الريش بمختلف نسب العرض على الضاغط الطرد المركزي المطور. علاوة على ذلك، فإن أداء ضاغط الطرد المركزي يعتمد على التوافق الصحيح بين ريشة الضاغط مع الناشر ذي الريش. بالإضافة إلى ذلك، أجريت مقارنة بين منحنيات الكفاءة البولوتروبيكية ونسبة الضغط الكلي والضغط الاستاتيكي والخصائص الأيروديناميكية لنسب العرض المختلفة. وايضا ، تم تحليل متجهات السرعة في ممرات تدفق الناشر ورقم ماخ المطلق والتدفق الثانوي في المقطع العرضي قرب مخرج الناشر بالتفصيل لنسب عرض 0.5 ، 0.7 ، 0.8 ، 1 و 1.2. وكان هدف آخر لهذا البحث هو لدراسة ومحاكاة تأثير الناشر ذي الريش على أداء الضاغط الطرد المركزي. أجريت المحاكاة باستخدام تحليل سي إف دي (أنسس CFX)

على التدفق الأيروديناميكي للتنبؤ العددي للأداء من حيث نسبة الضغط والكفاءة البولوتروبيكية ومعدل التدفق لطور الضاغط الطرد المركزي. النتائج التي تم الحصول عليها من سي إف دي حلت لفهم أفضل لتدفق السائل من خلال طور الضاغط الطرد المركزي، ونتيجة لذلك عندما يكون نسبة العرض 0.5، تدفق الجريان في ممرات الناشر يميل إلى أن يكون أكثر انتظاماً. الجريان العكسي والدوامات قرب سطح الضغط مختلفة، الدوامات وانفصال الجريان قرب سطح الامتصاص تكون متناقصة. استنتاجياً، لوحظ أن الكفاءة متزايدة ونسبة الضغط الكلي والضغط الاستاتيكي لنسبة العرض 0.5 كانت متزايدة.

NOMENCLATURE

CFD	Computational Fluid dynamics
CAD	Computer Aid Design
IGES	Initial Graphics Exchange Specification
TE	Trailing Edge
LE	Leading Edge
Pt	Total Pressure
Ps	Static Pressure
Pr	Pressure ratio
Tt	Total Temperature
Ts	Static Temperature
Mabs	Absolute Mach Number
Mrel	Relative Mach Number
Cm	Meridional Velocity
R	Blade Radius Location
Z	Blade Axial Location
k- ω -SST	K-Omega Turbulence Model
k- ϵ	k-Epsilon Turbulence Model
3D	Three Dimensions
W_1	Inlet Width Diffuser
W_2	Outlet Width Diffuser

1. INTRODUCTION

In these days, interest has more progressively been devoted to the development of turbochargers because of their compact size, large capacity, high performance, and ability to improve volumetric efficiency. Turbochargers are broadly used in many applications, such as marine, diesel engines, automobile engines, and small gas turbines for aircraft engines. The improvement of turbocharger compressor performance and the extension of the stable operating ranges are becoming critical for the viable future of low emission engines. In centrifugal compressor case, it is known that unsteady behaviour becomes apparent when the air mass flow through the compressor is lower than the critical level. This unstable phenomenon is denoted as a surge and corresponds to a backflow of compressed fluid through the compressor into its inlet. Generally, the performance of a centrifugal compressor is expressed as a relationship between the mass flow rate and the pressure ratio on a line with a constant number of revolutions.

Furthermore, the influences of the different diffuser meridian channel width ratios on the compressor performance under design conditions show a remarkable significance in terms of improving the efficiency of the whole machine in a micro gas turbine centrifugal compressor Yang [2011]. The effect of pulsating flow inside a centrifugal compressor and the corresponding pressure pulses on the compressor surge line can be very important because the pulsating flow is in the range of 40-67 Hz (corresponding to characteristic

pulsation when boosting an internal combustion engine) which increases the surge margin Galindo [2009]. The application of CFD to turbocharger compressor characteristic predictions over a range of speed, to develop an efficient methodology for analysing the turbocharger compressor performance, and to compare the computation versus rig measurements Baris [2011]. In addition, the stall flow phenomenon inside a turbocharger centrifugal compressor with a vaneless diffuser simulated numerically and the amplitude of the static pressure oscillation at this frequency in the diffuser is increased with the reduction in compressor mass flow, the results show that there is a distinct stall frequency at the given compressor speed Guo [2007]. The analytical model for the centrifugal compressor was proposed to predict the compressor performance such as outlet pressure, efficiency and losses. The model provides a valuable tool for evaluating the system performance as a function of various operating parameters Jiang [2006]. The compressor performance map is described experimentally for characterization of the automotive turbocharger, and a mathematical tool has been developed for marking out surge operation points from stable compressor points Galindo [2006]. The contribution to the design methodology and performance assessment of low solidity vaned diffusers to understand the pressure recovery phenomena in each of the three types of diffusers, and the effect of design parameters on performance was studied by Engeda [2003]. The effect of impeller exit width trimming was studied and discussed along with the effect on overall performance on the basis of experimental data for two impellers. One with a low flow coefficient and the other with a high flow coefficient, blade loading and impeller diffusion was examined by Engeda [2007].

The stable working conditions and surge phenomena were simulated and boundary was used as the Method of Characteristics to determine the flow conditions at compressor inlet and outlet. To downsize the engine displacement to increase the power output and to reduce fuel consumption Galindo [2010]. The complex shock waves within the diffuser throat and impeller inlet, respectively, within high-speed compressors. These flow phenomena does not occur in low speed compressors and are very significant in the design of these compressors Cukurel [2010] and Higashimori [2004]. Many researchers have indicated that suitable treatments can extend the stable operating range of a turbocharger centrifugal compressor, but the performance is still insufficient under the majority of conditions.

The aerodynamic performance of centrifugal compressors is bound by surge and chokes on a compressor performance map. Much effort has been spent to define performance maps Shook [1995] and Layth [2014] to determine the performance of a new high speed compressor. The barrier imposed by the surge line, which separates the regions of stable and unstable operation, is of particular interest due to its close proximity to the maximum efficiency operating point. The initiation of unstable operation has been studied by many researchers Gravdahl [2004]. When the mass flow through the compressor is below the surge line, unstable operation occurs in the form of rotating stall or surge.

One of the important aspects of designing efficient compressors is properly matching the impeller and diffuser. The importance of this topic was presented by Ziegler [2003] who showed that the presence of diffuser vanes considerably increases the pressure at the exit of the impeller, proving that there is a coupling between the impeller and diffuser. The diffuser used in the compressor must be designed for the mass flow rate, flow velocities, and flow angles at the exit of the impeller. This can be very challenging due to the highly unsteady nature of compressors and the jet-wake flow at the exit of the impeller. The performance of the impeller and diffuser is highly coupled, as shown by Ramakrishnan [2007]. The potential field generated by the diffuser acting on the impeller exit flow field is not only driven by geometry but is also dependent on the unsteady

diffuser loading. The potential field is the effect the geometry that it has on the pressure in the airflow. This diffuser loading is in turn a function of the rotating impeller potential field and the highly three-dimensional velocity field produced by the impeller. The diffuser potential field acting on the impeller has been studied using CFD by Barry [1991]. Within the impeller passage, there are high and low momentum regions known as the jet and wake, which have been studied by Gallier [2007]. These zones not only vary along the circumference of the impeller, but also along the span, from the hub to the shroud. As flow emerges from the impeller, the blade forces on the fluid are lost, and the jet and wake regions undergo rapid mixing within the vaneless space. The design of the vaneless space has a significant impact on the overall performance of the compressor, including operating range, stability limits, viscous loss, and diffuser separations. Some of the earlier models based on low-speed compressors showed complete mixing within the vaneless space. Investigations on high-speed machines, such as in Ziegler [2007], have shown that the mixing process is not sufficient to produce a uniform flow field at the leading edge of the diffuser. The flow at the inlet of the diffuser is made up of shocks, partial separations, varying momentum and incidence angles. The interaction between the diffuser and impeller makes it difficult and impossible to predict the behavior of these flow irregularities and to study one isolated from the other respectively. The degree of these impeller-diffuser interactions is highly dependent on the radial gap between the impeller exit and diffuser inlet along with the diffuser vane geometry. Due to this dependence, it is important for the designer to understand the effects of these geometries in order to properly match these components. The angle of the diffuser vanes is also an important aspect of the performance due to the varying incident angles occurring at the diffuser inlet because of the unsteady flow at the exit of the impeller. There are several studies that have been conducted on the effects of radial gap and vane angle such as the work of Ibaraki [2007]. In the light of the facts given above, the work reported in this paper deals with numerical investigations on interaction of vaned diffuser with modified centrifugal compressor impeller where CFD simulations and flow behavior of each conventional and modified centrifugal compressor impeller with vaned diffuser configurations were performed. In this paper, the study is focused on the effect of different diffuser meridional passage width ratios on the compressor performance to achieve high quality flow and further performance improvement of the turbocharger compressor.

2. DESIGN & SPECIFICATIONS

The compressor studied was a centrifugal compressor with vaned diffuser stage model. The inflow and the outflow of the fluid zone were as shown in Figure 1. under the same geometric conditions except for meridional passage width, keeping the diffuser meridional passage inlet W_1 unchanged, changing the outlet width W_2 selecting, a different width ratio of the diffuser meridional passage $W_2/W_1=0.5, 0.7, 0.8, 1$ and 1.2 respectively. The main geometry features it's was from a unique geometry model TD04-10T4 turbocharger. The dimensions of the modified compressor vaned diffuser are given in Table 1.

Figure 2 shows the geometry of the modified compressor wheel vaned diffuser stage comprising of six main impeller blades, 12 splitter blades and 19 diffuser vanes. The CFD computations for the modified designs were performed on the geometries. All the surface geometry, inlet, exit, and periodic boundaries, were defined via computer-aided design (CAD) as Initial Graphics Exchange Specification (IGES) parts.

3. CFD METHODOLOGY

3.1 Grid Generation

The surface mesh is generated by using a re-triangulation mesh on the impeller and splitter surfaces. The surface repair tools have sufficient control to allow the analysis by choosing among the components to include and exclude in the meshing. This is to control the size of the triangulations in various parts by using surface curvature or by defining local refinement zones. Once these surface mesh control settings are defined, the tool retains the association with the imported CAD parts. This makes parametric modelling of the components very easy. The volume mesh is generated by using a polyhedral, as validated for flow and thermal solutions Peric [2004] and Mendonca [2008]. The polyhedral cell mesh consists of 12-16 faces, agglomerated from the underlying automatically generated tetrahedral mesh. Polyhedral meshes offer significant advantages over traditional mesh types. Like tetrahedral and unlike hexahedral meshes, they can be automatically generated. Polyhedral meshes exhibit far less numerical diffusion compared to tetrahedral meshes because of the greater likelihood of face alignment to the flow. Gradient calculations are more accurate due to the greater number of face neighbours. Cell counts are typically a third of the equivalent tetrahedral meshes for similar fineness of resolution. It all means that polyhedral meshes run faster, are more accurate and converge more robustly than tetrahedral meshes Peric [2004]. The computational grid, for the modified impeller blade passage with two splitters comprising exactly 442035 structured hexahedral elements in multi-block environment, for the vaned diffuser passage comprising 363300 hexahedral elements were generated using TurboGrid. Sufficiently fine grid elements were created in the impeller tip clearance region, around the impeller, and at the hub and shroud walls, as shown in Figure 3. Sufficient mesh quality checks were performed by keeping the parameters like mesh angle and determinants within acceptable limits.

3.2 Fluid Flow Modelling

The fluid zone comprises of one area enveloping all the rotating parts (blades and hub) and the other area of the stationary parts (shroud, inlet, outlet and vaned diffuser). The left and right boundaries are defined as periodic. Turbulence is modelled using the $k-\omega$ -SST model. This model is a zonal combination of $k-\omega$ near the wall, nominally in the boundary layer, and $k-\epsilon$ away from the walls. When the near-wall mesh is compatible with the wall-function approach, this model behaves predominantly as a high-Reynolds number $k-\epsilon$ formulation. All surfaces are treated as adiabatic. Total pressure and total temperature are applied to the inflow inlet boundary. The outflow outlet condition is set to static pressure. The exit static pressure is modified in stages, and a new analysis is run to determine the mass flow rates. The exit pressure is adjusted from the surge to the choke limit to give constant speed compressor performance curves.

3.3 Boundary Conditions Used in Simulation

Boundary conditions specification is an essential part in using CFD. They vary from symmetric to periodic, from wall to another, and from inlet to outlet. As was mentioned earlier specifying the boundary conditions is a pre-processing process. The boundary conditions used in this work are as shown in Figure 4 and listed in table 2:

4. RESULTS

The numerical method used by the solver part of the software requires an iterative process in order to obtain a solution. In general, the residual magnitude should decrease as

the solution converges. When the magnitude of the residuals for all the quantities falls below the convergence level, the solver will stop iterating, and the results will be exported for post-processing. Figure 5 shows the total-total Polytropic efficiency and total-total pressure ratio with respect to width ratio curves, considering the best performance was at 0.5 width ratio, and the worst one was at 1.2 width ratio. Moreover, it is clearly seen that the width ratio does have an important impact on the efficiency and pressure ratio. The reason might be due to its own characteristics of this type of centrifugal compressor.

The results are compared with experimental work data which was presented for validation Jawad [2014]. Figure 6 shows the predicted compressor characteristic at the four speeds investigated versus the rig measurements. The calculations at low pressure ratio points for all speeds correspond very closely in predicting mass-flow to the measurements. At the high speed line, the 60,000 and 80,000 RPM predictions are in good agreement with the experiments, whereas at the highest speed, 100,000 RPM deviation from the measurements of 3-5% is observed. At the higher pressure ratios, and especially near the surge line, the deviation is up to 4.5% over-prediction at any given speed. It is found that the behaviour of low pressure ratio point for a corresponding specific speed very closely to the experimental work data as shown in figure 6 .

Figure 7 shows the meridional velocity difference across the trailing edge (TE) Spanwise of the centrifugal compressor impeller configurations for a different width ratio it is clearly seen that meridional velocity is increasing at mid Spanwise between hub and shroud, and then it is decreasing at a shroud, the reason due to tip clearance between shroud and impeller tip.

Figure 8 shows the meridional velocity difference across the trailing edge (TE) Spanwise of the vaned diffuser configurations for a different width ratio it is clearly seen that meridional velocity is increasing at 0.2 spanwise between hub and shroud, and then it is decreasing at a shroud, the reason due to narrow passage between shroud and vaned tip. Obviously, the meridional velocity at 0.5 width ratio is the higher than the others' types, the reason behind that due to an outlet narrow passage between shroud and vaned tip.

Figure 9 shows the relative Mach number difference across the trailing edge (TE) Spanwise of the centrifugal compressor impeller; it is clearly seen that relative Mach number is decreasing for the 0.5 width ratio than others' width ratios.

Figure 10 shows absolute Mach number difference across the Spanwise location at trailing edge of the vaned diffuser; it is visibly seen that Mach number is higher at 0.5 width ratio than others' types of width ratios.

Figure 11 shows absolute Mach number difference across the streamwise location, from inlet impeller to outlet vaned diffuser; it is visibly seen that Mach number is higher at space between impeller exit and vaned inlet; therefore, it is very important to take into account the impact of a space ratio in design.

Figure 12 shows the static pressure difference across the streamwise location of the modified vaned diffuser centrifugal compressor for a different width ratio; it is clearly seen that the static pressure is decreasing at space between exit impeller and inlet vaned diffuser; moreover, it is obviously seen that static pressure is increasing through vaned diffuser due to the kinetic energy which is converted into static pressure. Conclusively, the static pressure for 0.5 width ratio is the higher than others' types of width ratios.

Figure 13 shows the velocity vectors magnitude at mid spanwise location for impeller vaned diffuser configurations in clockwise rotation from the impeller inlet and vaned exit. It can be seen that the flow conditions in diffuser near the outlet vary obviously under different width ratio, when the width ratio is 1.2, as a result of meridional passage, a backflow vortex exists near the pressure surface next to the diffuser outlet. It greatly increased the flowing loss; therefore, the efficiency and pressure ratio is low; when the

width ratio is 0.8, the backflow vortex and its influence region decrease a lot, when the width ratio is 0.5, the flow field becomes uniform. Therefore, the flow losses decrease while the efficiency and pressure ratio becomes higher.

Figure 1 4 shows the contour of relative Mach number at mid spanwise location for impeller vaned diffuser configurations from the impeller inlet and vaned exit, as an example of CFD computations. It can be seen no choke of flow at the inlet of the modified type because of the uniform distribution of the throat area between blade to blade passages. If we extend the leading edge of the splitters to the leading edge of the full blade, it will minimize the throat area and cause choking. It can be seen the flow in the space area between the trailing edge of the impeller, and the leading edge of the vanes' diffuser which is close to Mach one meaning the space area ratio which is a very important factor to modify in order to remove any choking of the flow for all configurations of width ratios. It is clearly seen that the effect of flow vaned angle to increase and decrease the backflow vortex.

Figure 1 5 shows the contour of static pressure difference on the meridional surface of the impeller vaned diffuser from the inlet to outlet location for different configurations of width ratios; it is obviously seen that the effect of outlet vaned width of the distribution of static pressure, it can be seen evidently the effect of vaned diffuser to increase the static pressure, the reason behind that due to the kinetic energy which is converted into static pressure.

Figure 1 6 shows the relative Mach number on a meridional surface of the impeller vaned diffuser from the inlet to outlet location for different configurations of width ratios. It is clearly seen that the relative Mach number of 0.5 width ratio type is lower than relative Mach number of other's types at outlet flow and at the space between impeller exit and vaned outlet. It is necessary to convert the high kinetic energy to a static pressure through a diffuser provided downstream of the impeller.

Figure 1 7 shows the contour of meridional velocity from Leading Edge (LE) of impeller to Trailing Edge (TE) of vaned diffuser for different configurations of a width ratio. It is clearly seen that the effect of outlet 0.5 width ratio to decrease the meridional velocity along a meridional length of vaned diffuser. Moreover, the diffuser is used to reduce this velocity while at the same time it increases the static pressure. It can be seen that the high velocity is located at space between impeller exit and vane's inlet. As earlier mentioned that the space area ratio which is a very important factor to modify. The numerical analysis was carried out including the impeller vaned diffuser flow passage only. The results show the effect of the outlet width ratio vaned diffuser on the performance of centrifugal compressor. The modification of a previous design of centrifugal compressor impellers gives a better performance or a wide operating range. CFD models give a much deeper understanding of the flow inside a vaned diffuser centrifugal compressor, enabling us to solve many problems easily and rapidly.

5. CONCLUSIONS

Steady state flow simulations have been conducted in order to analysis, the effects of the different meridional passage width ratio of vaned diffuser on the centrifugal compressor performance are systemically simulated and analysed. The Parametric computations were performed on a 3D-Turbulent CFD to obtain the performance of backswept impeller configurations at a certain speed; it was 50k RPM. The analysis of the flow characteristics was also performed to obtain a better understanding of the blade to blade vaned diffuser compressor behaviours. The results show the range of the best width ratio is determined. The following conclusions are obtained; firstly, reducing the width

ratio can enhance the performance of centrifugal compressor. When the width ratio is 0.5, the Polytropic efficiency of the impeller coupled with the vaned diffuser reaches the highest value 73.52%, and the total pressure ratio gets to the highest value 1.35. secondly, as the width ratio decrease, the flow in radial direction of the diffuser meridional passage is squeezed. The backflow and vortex near the pressure surface gradually disappear. The flow tends to be uniform; hence the efficiency and total pressure ratio are both improved. An effort was made to model the flow from the inlet to the exit of a centrifugal compressor stage consisting of all the components in place using CFD tools. The vector plots, contour plots and Stream line plots are generated for better understanding of fluid flow through centrifugal compressor stage. Conclusively, the aerodynamic results show that the best width ratio range of diffuser meridional passage is 0.5 and 0.7. Obviously, the performance was significantly affected by outlet meridional width passage vaned diffuser.

Table 1: Geometric Features of the Vaned Diffuser Centrifugal Compressor.
(ANSYS BLADE DESIGN)

Centrifugal Compressor	Modified (Double Splitter)
Axial Width of Impeller in Meridional View	30 mm
Inner Radius at Compressor Inlet	8 mm
Outer Radius at Compressor Inlet	35 mm
Impeller Outer Radius	49 mm
Impeller Width at Trailing Edge	6 mm
Number of Blades	18
Number of Splitters	12
Tip Clearance at Shroud	95% Span
Splitter1 angular offset (pitch fraction or location)	67%
Splitter2 angular offset (pitch fraction or location)	33%
Number of Diffuser Vanes	19
Vane Inner Radius	61 mm
Vane Outer Radius	82 mm
Vane Inner Axial Width	6 mm
Vane Outer Axial Width	4 mm
Vane Outer Flow angle	30°
Inlet Width Diffuser (W_I)	6mm

Table 2: Boundary Conditions Used in CFD Calculations.

Flow angle at domain inlet (degree)	(0) Radial Direction
Total temperature at domain inlet (Kelvin)	303
Total pressure at domain inlet (bar)	1.03
Rotational speed (rpm)	50000
Physical Timescale	0.00002
Number of Iteration	100
Stator's Outlet-Rotor's Inlet	General Connection (Stage)
Flow Direction	Cylindrical (1,0,0)

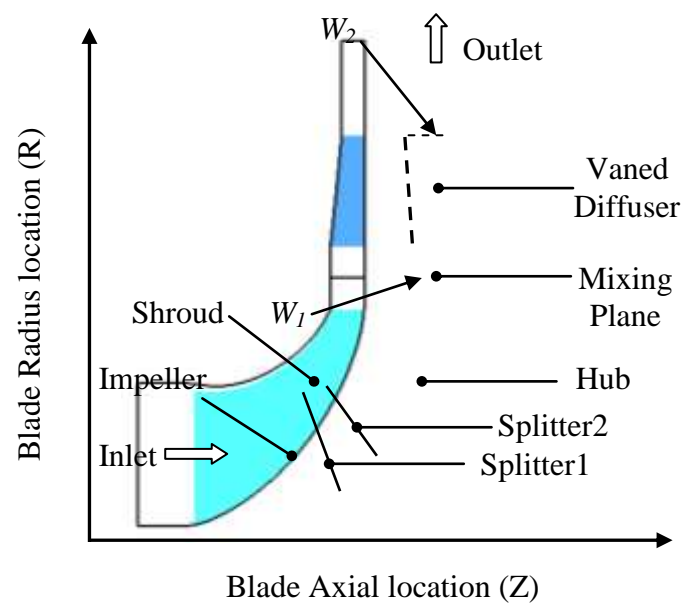


Figure 1: Meridional View of the Impeller, Vaned Diffuser, Hub and Shroud.

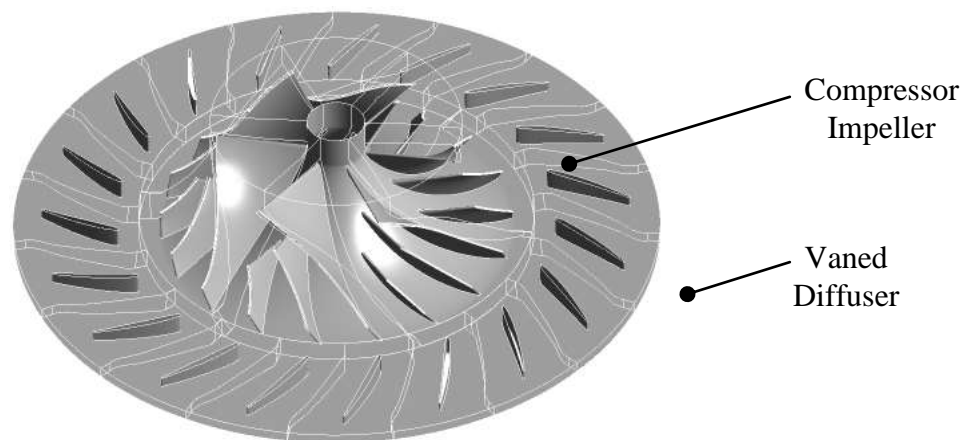


Figure 2: Isometric 3D View of Modified Vaned diffuser Centrifugal Compressor stage.

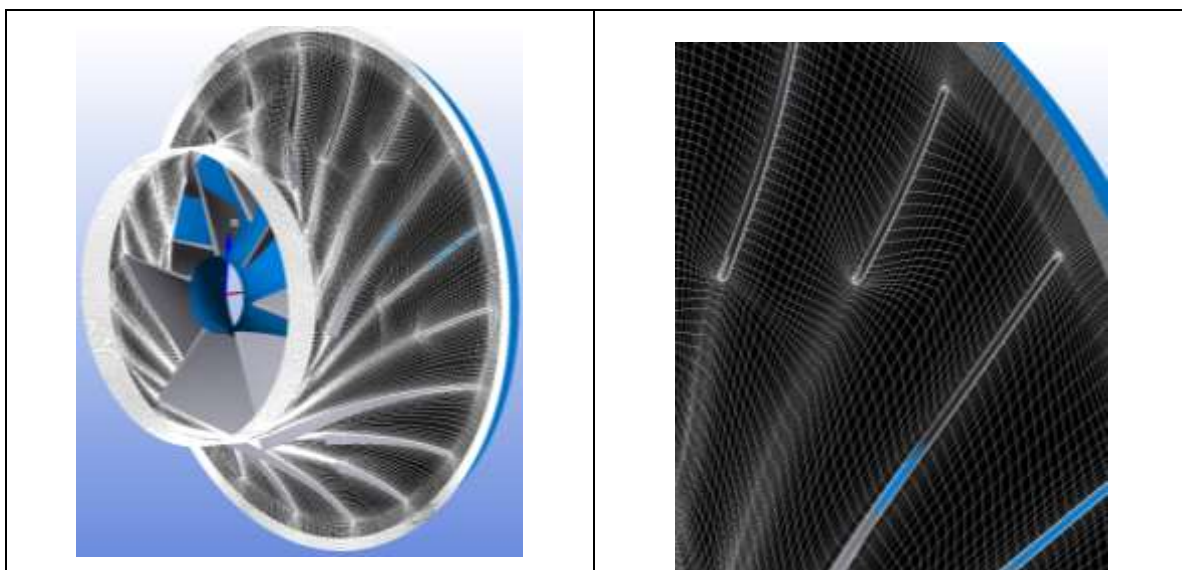
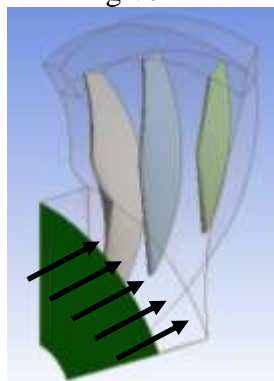
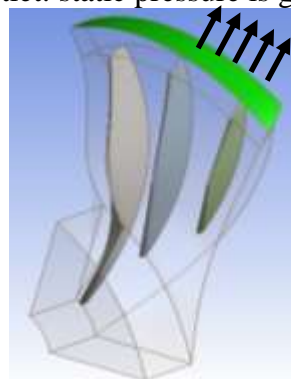


Figure 3: Blade to Blade That is Used in the Simulation

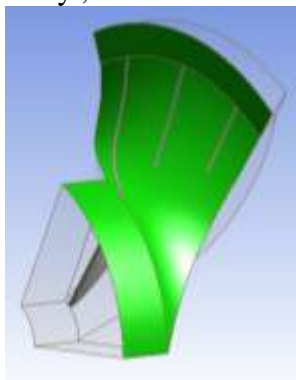
Inlet: the pressure and temperature are given



Outlet: static pressure is given



Wall (stationery), which is none moving boundary , this is called shroud



Wall (moving), which is the hub and blade boundary condition



Figure 4: Boundary conditions specification

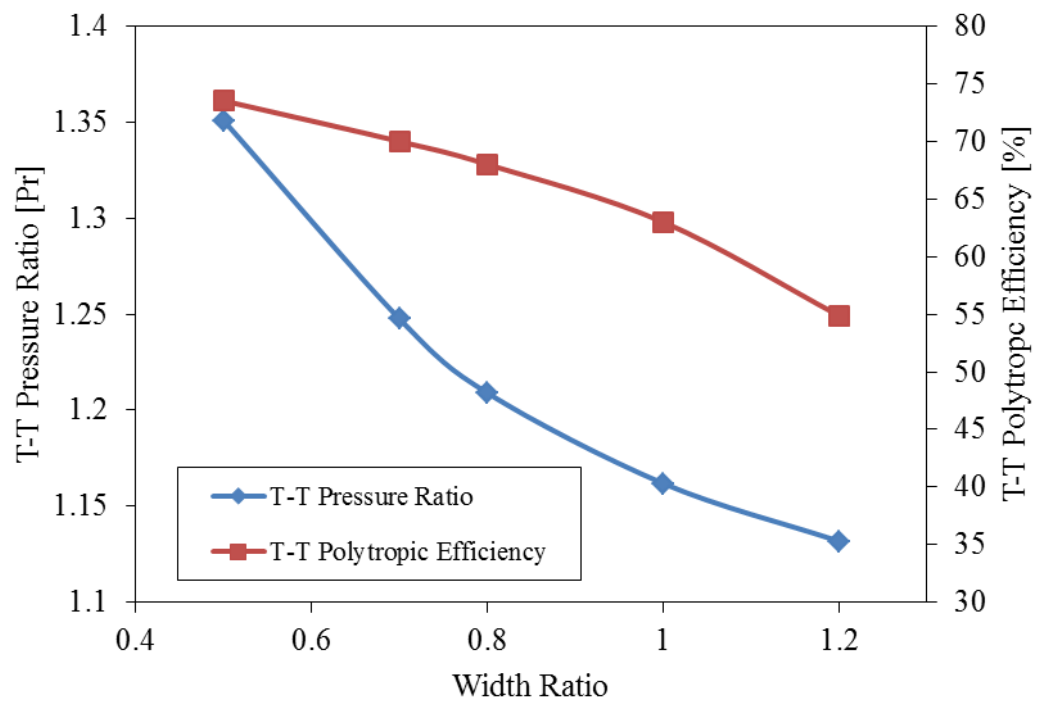


Figure 5: Relationship between the Total-Total Polytypic Efficiency and Total-Total Pressure with Width Ratio at 50% span.

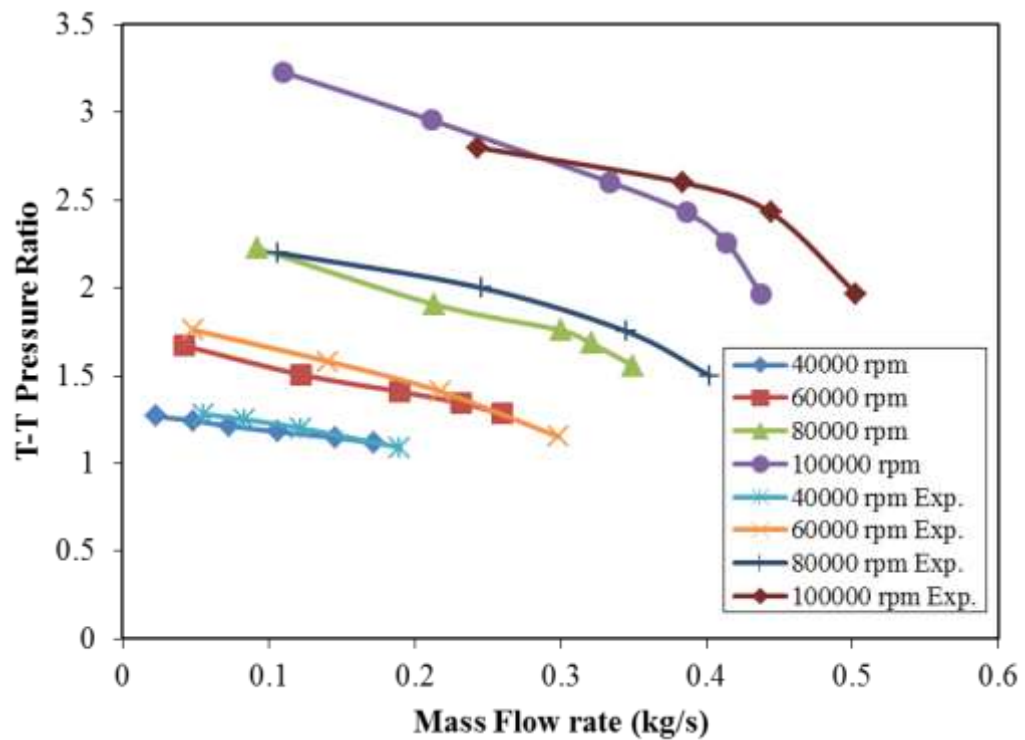


Figure 6: Comparison of Experimental With Numerical Work for Conventional Type

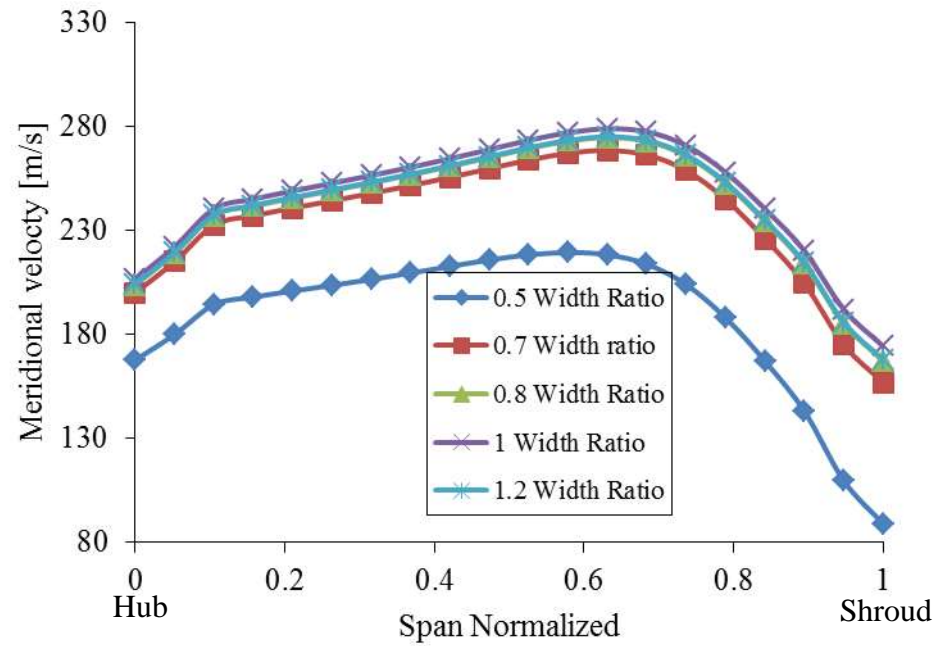


Figure 7: Relationship between the Meridional Velocity (C_m) and Span Normalized at Trailing edge (TE) of Impeller for Different Width Ratio.

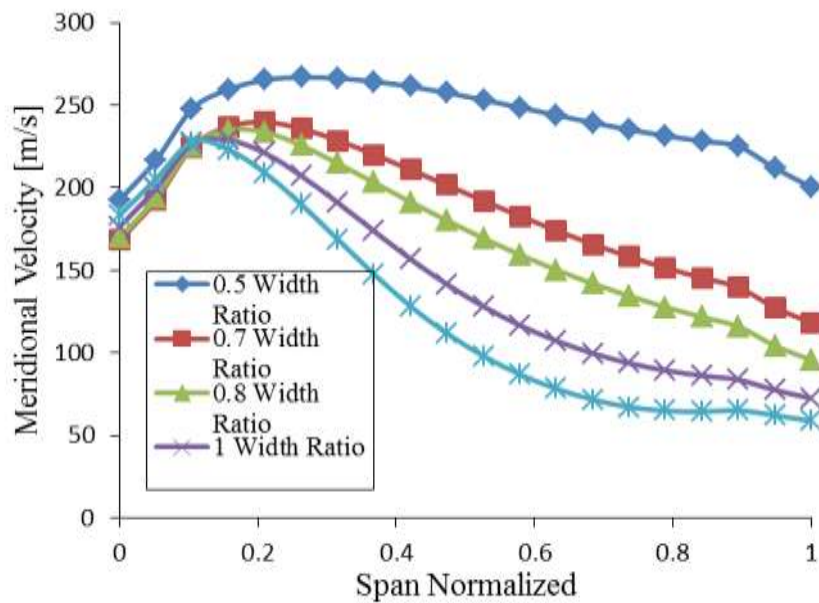


Figure 8: Relationship between the Meridional Velocity (C_m) and Span Normalized at Trailing edge (TE) of Vaned Diffuser for Different Width Ratio.

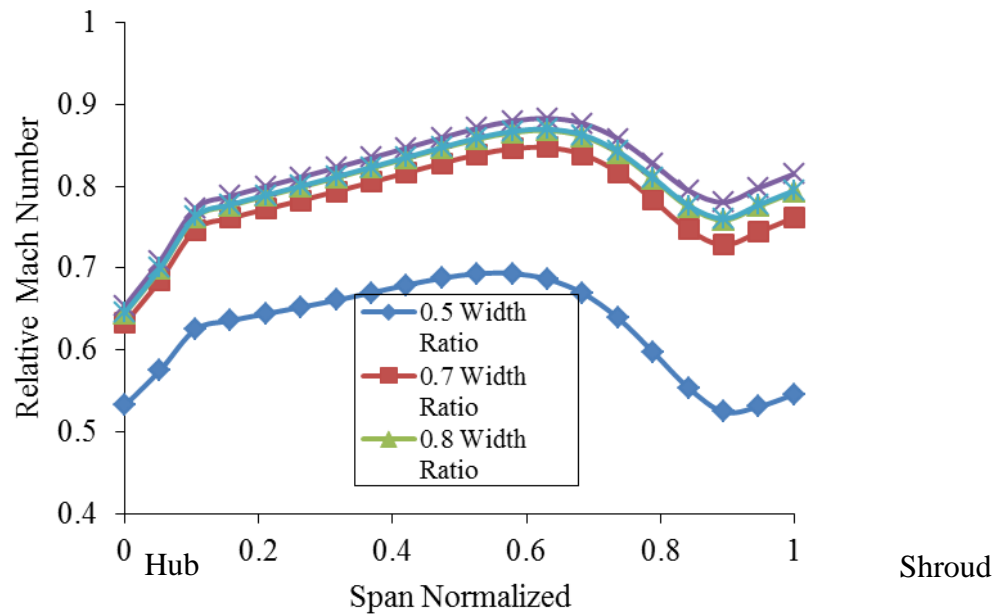


Figure 9: Relationship between the Relative Mach Number (M_{rel}) and Span Normalized at Trailing edge (TE) of Impeller for Different Width Ratio.

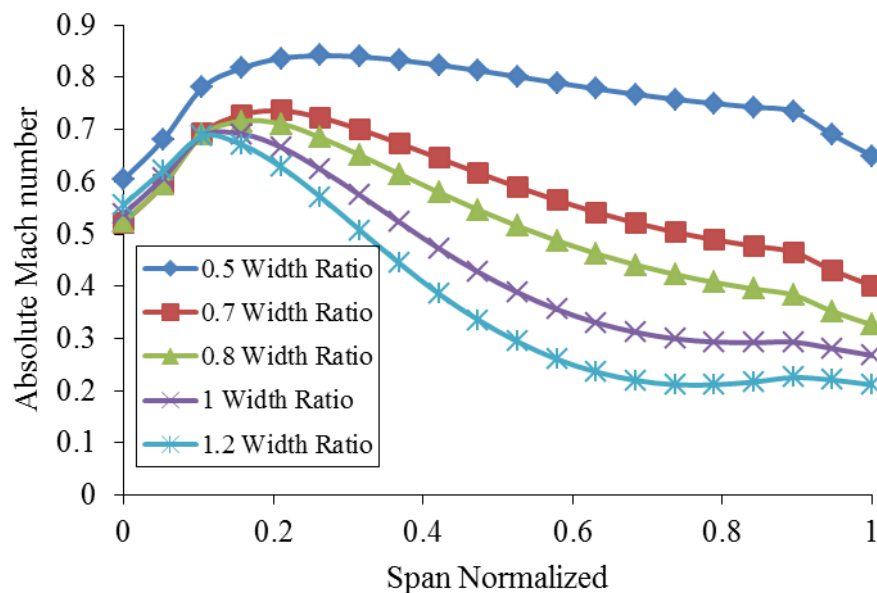


Figure 10: Relationship between the Absolute Mach number with Spanwise Location at Trailing Edge (TE) of Vaned Diffuser.

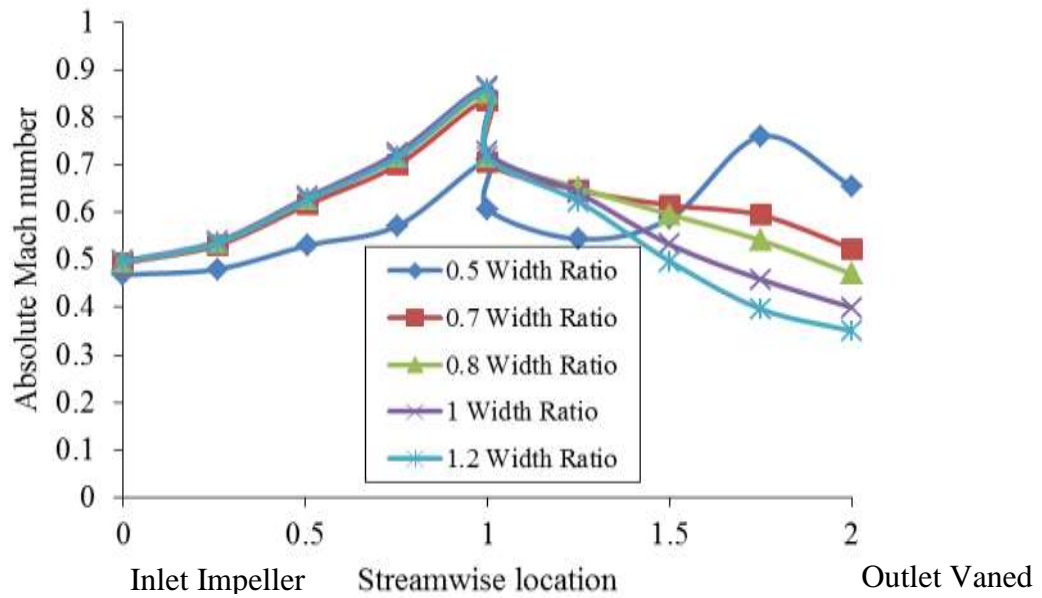


Figure 11: Relationship between the Absolute Mach number with Streamwise Location from Inlet to Outlet.

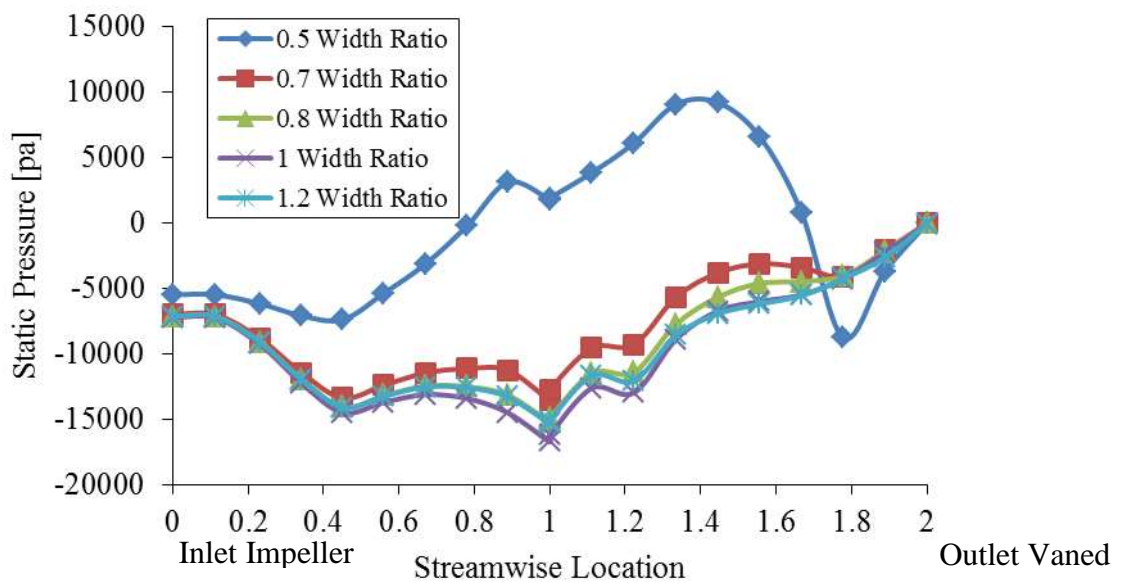


Figure 12: Relationship between the Static Pressures (Ps) with Streamwise Location (Inlet-Outlet).

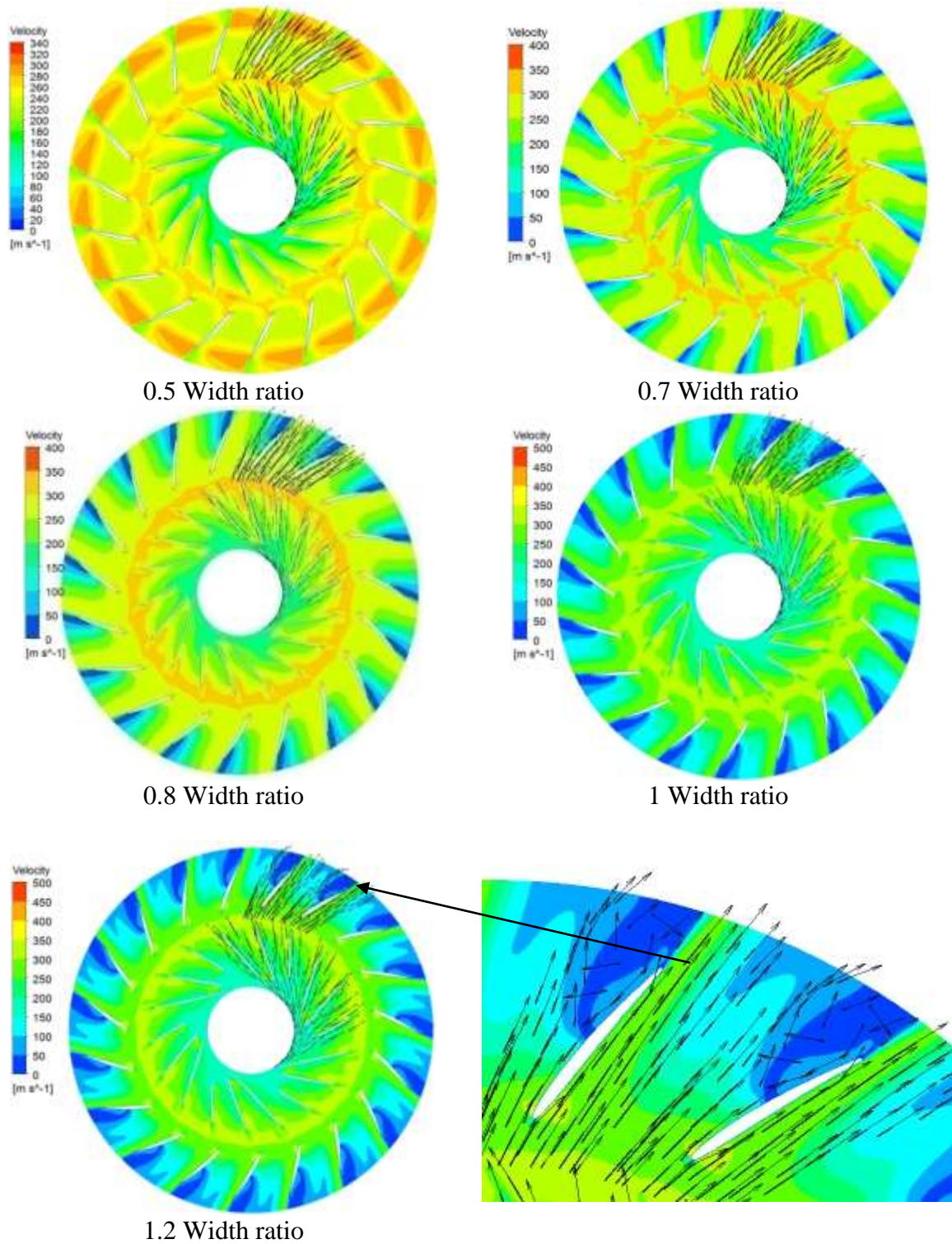


Figure 13: Velocity Vectors at 50% Span Position for Different Width ratio of Vaned Diffuser

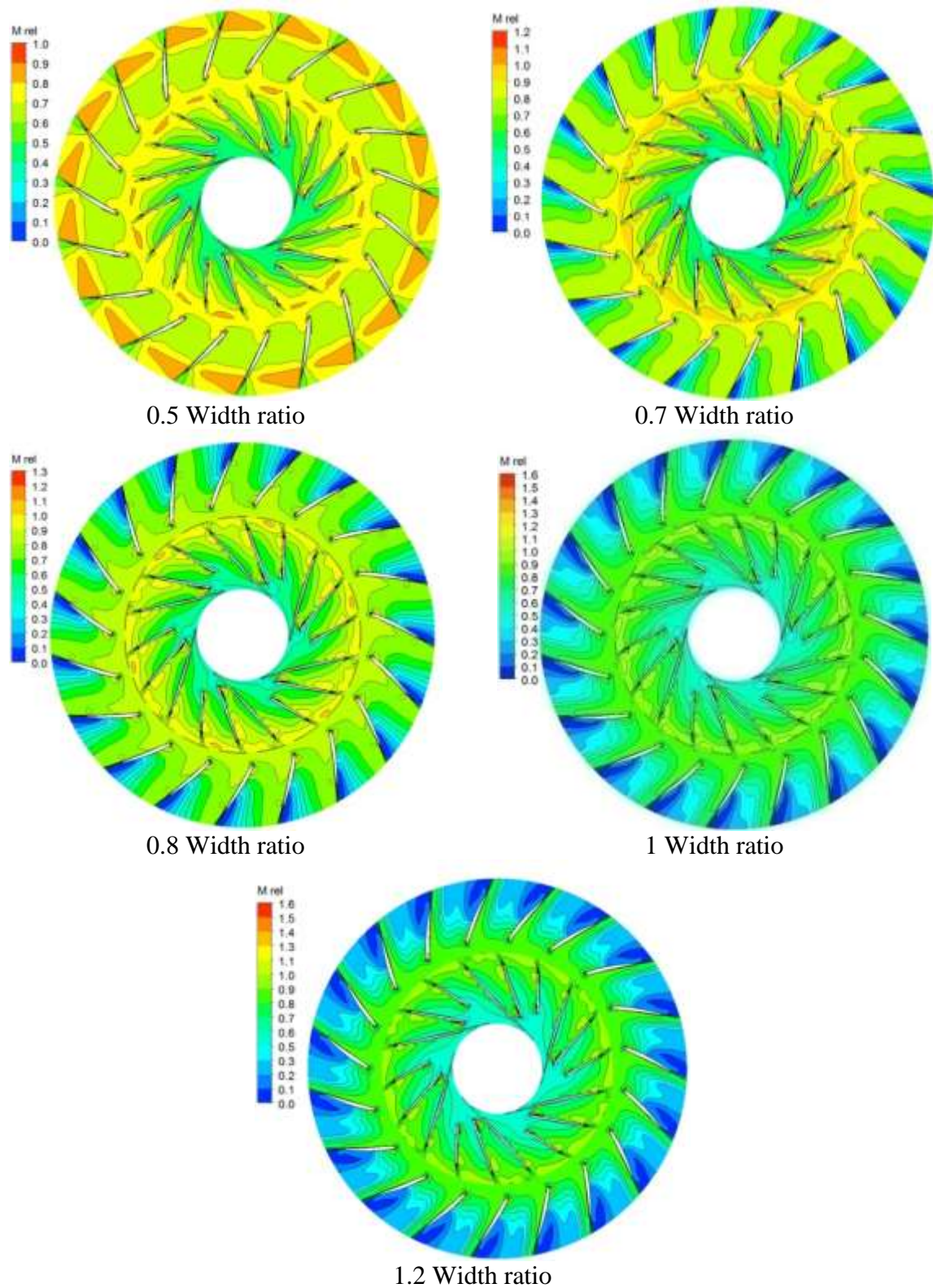


Figure 14: Contour of Relative Mach number at 50% Span Position for Different Width ratio of Vaned Diffuser.

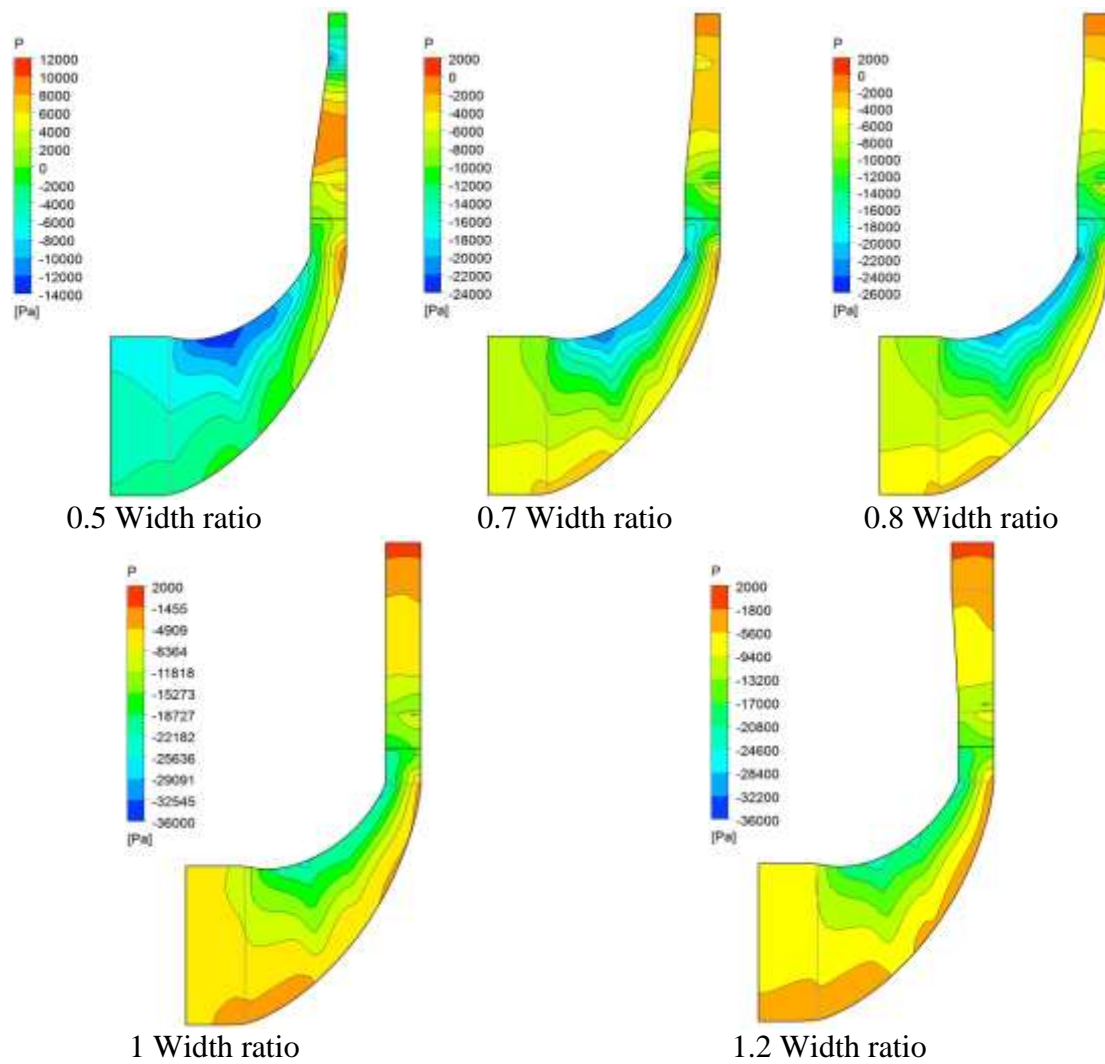


Figure 15: Contour of Static Pressure on Meridional Surface for Different Width ratio of Vaned Diffuser

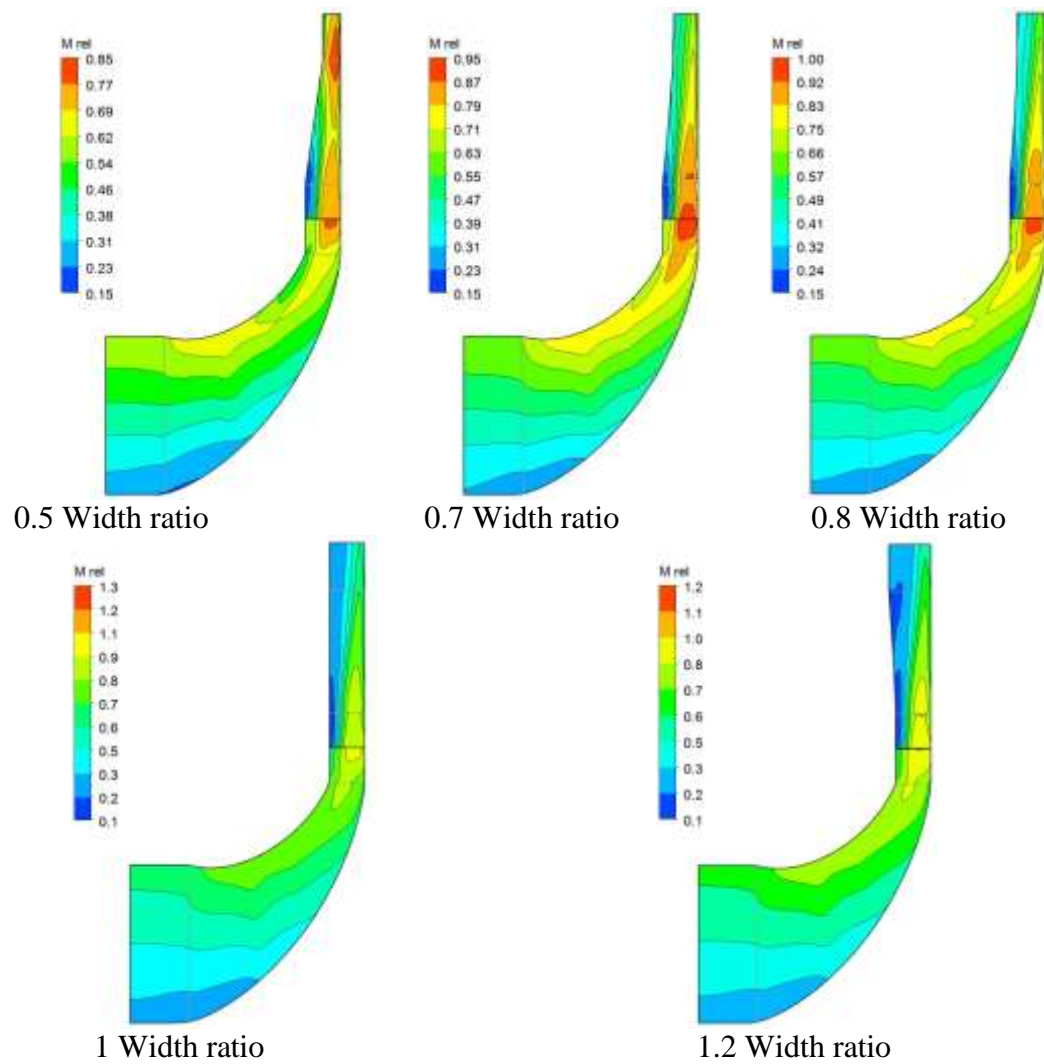


Figure 16: Contour of Relative Mach number on Meridional Surface for Different Width ratio of Vaned Diffuser.

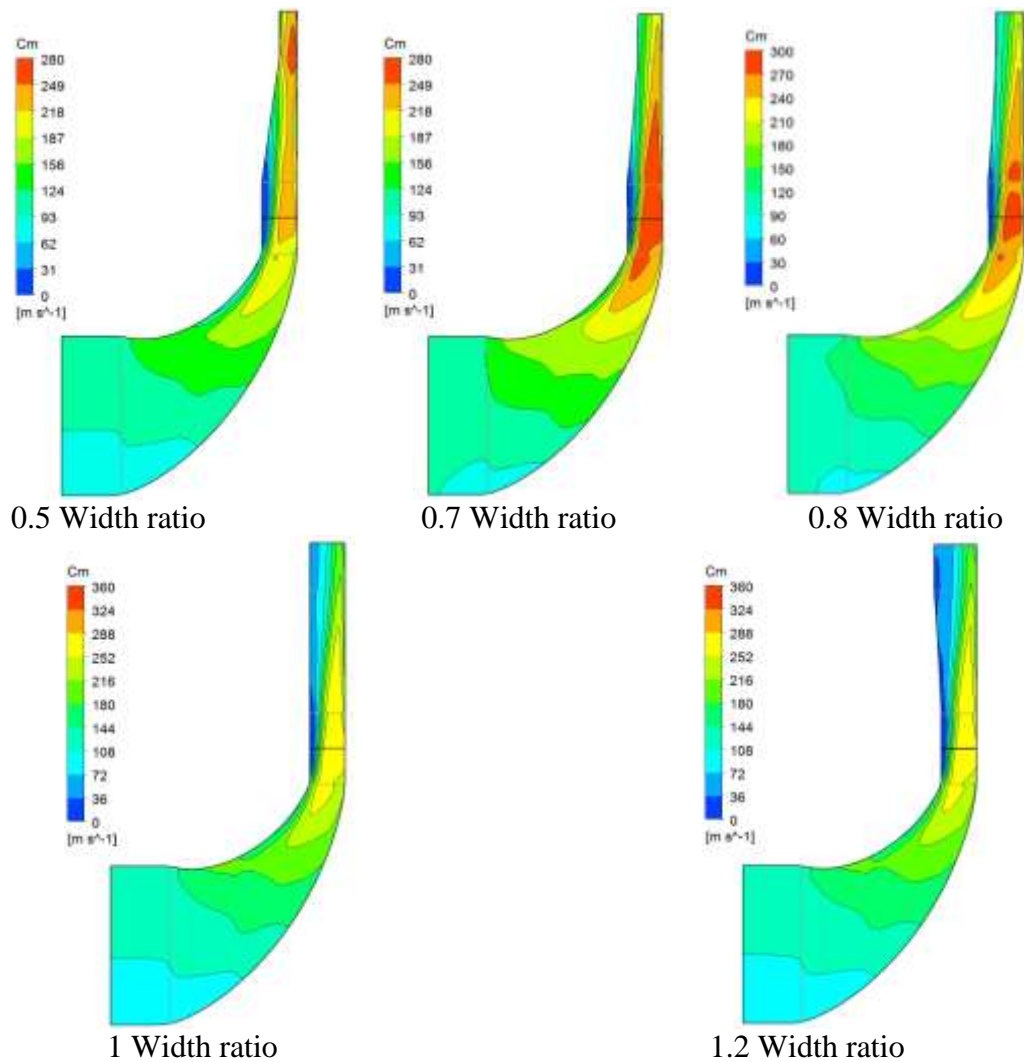


Figure 17: Contour of Meridional Velocity on Meridional Surface for Different Width ratio of Vaned Diffuser.

REFERENCES

- A. Engeda (2003). Experimental and numerical investigation of the performance of a 240 kW centrifugal compressor with different diffusers. *Experimental Thermal and Fluid Science*, 28:55-72.
- A. Engeda (2007). Effect of Impeller Exit Width Trimming on Compressor Performance. *Proceedings of the 8th International Symposium on Experimental and Computational Aerothermodynamics of Internal Flows*. ISAI8- 00135.
- B. Cukurel, P.B. Lawless, and S. Fleeter, 2010. Particle Image Velocity Investigation of a High Speed Centrifugal Compressor Diffuser, Spanwise and Loading Variations. *Journal of Turbomachinery*, vol. 132, pp. 1-9.
- H. Higashimori, K. Hasagawa, K. Sumida, and T. Suita, 2004. Detailed Flow Study of Mach number 1.6 High Transonic Flow with a Shock Wave in a Pressure Ratio 11 Centrifugal Compressor Impeller. *Journal of Turbomachinery*, vol. 126, pp. 473-481.

- J.T. Gravdahl and F. Willems, 2004. "Modeling of Surge in Free-Spool Centrifugal Compressors: Experimental Validation," *Journal of Propulsion and Power*, vol.20, pp. 849-857.
- J. Galindo, H. Climent, C. Guardiola, A. Tiseira (2009). On the effect of pulsating flow on surge margin of small centrifugal compressors for automotive engines. *Experimental Thermal and Fluid Science*, 33:1163–1171.
- J. Galindo, J.R. Serrano, C. Guardiola, and C. Cervello (2006). Surge limit definition in a specific test bench for the characterization of automotive turbochargers. *Experimental Thermal and Fluid Science* 30 (2006) 449–462.
- J. Galindo, F.J. Arnau, A. Tiseira and P. Piqueras (2010). Solution of the turbocompressor boundary condition for one-dimensional gas-dynamic codes. *Mathematical and Computer Modelling* 52 (2010) 1288_1297.
- K.U. Ziegler, H.E. Gallus, and R. Niehuis, "A Study on Impeller-Diffuser Interaction-Part I: Influence on the Performance," *Journal of Turbomachinery*, vol. 125, 2003, pp. 173-182.
- K. Ramakrishnan, P.B. Lawless, and S. Fleeter, "High Speed Centrifugal Compressor Aeromechanics - Impeller Unsteady Aerodynamics," AIAA 2007-5020, Cincinnati, OH: AIAA, 2007, pp. 1-18.
- K. Gallier, P.B. Lawless, and S. Fleeter, "PIV Characterization of High Speed Centrifugal Compressor Impeller-Diffuser Interaction," AIAA 2007-5019, Cincinnati, OH: AIAA, 2007, pp. 1-8.
- K.U. Ziegler, H.E. Gallus, and R. Niehuis, "A Study on Impeller-Diffuser Interaction-Part II: Detailed Flow Analysis," *Journal of Turbomachinery*, vol.125, 2003, pp. 183-192.
- Layth H. Jawad, S. Abdullah, R. Zulkifli and W.M.F.W. Mahmood, (2014). Numerical Study on the Effect of Interaction Vaned Diffuser with Impeller on the Performance of a Modified Centrifugal Compressor. *Journal of Mechanics* Vol. 30, April 113-121.
- M. Peric, (2004). Flow simulation using control volumes of arbitrary polyhedral shape. *ERCOFTAC Bulletin* 62.
- Mendonça F, Clement J, Palfreyman D and Peck A, (2008). Validation of Unstructured CFD Modelling Applied to the Conjugate Heat Transfer in Turbine Blade Cooling. ETC-8-198, European Turbomachinery Conference, Graz.
- O. Baris (2011). Automotive turbocharger compressor CFD and extension towards incorporating installation effects. *Proceedings of ASME Turbo Expo 2011: Power for Land, Sea and Air GT2011*.
- Q Guo, H Chen, X-C Zhu, Z-H Du, and Y Zhao (2007). Numerical simulations of stall inside a centrifugal compressor. *Power and Energy IMechE* Vol. 221 Part A: J.
- R. M. P.J. Shook, W. Oakes, 1994. "The Aerodynamic Performance of a High Speed Research Centrifugal Compressor Facility," *AIAA Paper 1994-2798*, pp. 1-9.
- S. Ibaraki, T. Matsuo, and T. Yokoyama, "Investigation of Unsteady Flow Field in a Vaned Diffuser of a Transonic Centrifugal Compressor," *Journal of Turbomachinery*, vol. 129, 2007, p. 686.
- W. Jiang, Jamil Khan, and Roger A. Dougal (2006). Dynamic centrifugal compressor model for system simulation. *Journal of Power Sources* 158 (2006) 1333–1343.
- W.B. Barry, "An Investigation of Unsteady Impeller-Diffuser Interactions in a Centrifugal Compressor," *Purdue University Thesis*, 1991.
- Y. Yang, Rong Xie, Lu-yuan Gong and Yang Hai (2011). Study of Influence of Diffuser Meridian Channel Shape on Performance of Micro-Gas Turbine Centrifugal Compressor. *Power and Energy Engineering Conference (APPEEC)*, 2011 Asia-Pacific 978-1-4244-6255-1/11.